Scandium Iridium Boride $Sc_3Ir_5B_2$ and the Quaternary Derivatives $Sc_2MIr_5B_2$ with M = Be, Al, Si, Ti, V, Cr, Mn, Fe, Co, Ni, Cu, Ga, or Ge: Preparation, Crystal Structure, and Physical Properties

E. A. Nagelschmitz and W. Jung*

Institut für Anorganische Chemie der Universität Köln, Greinstrasse 6, D-50939 Köln, Germany

Received April 17, 1998. Revised Manuscript Received July 22, 1998

The new compounds $Sc_3Ir_5B_2$ and $Sc_2MIr_5B_2$ with M = Be, Al, Si, Ti, V, Cr, Mn, Fe, Co, Ni, Cu, Ga, or Ge were prepared by arc-melting appropriate compressed mixtures of the elemental components in an argon atmosphere. They crystallize tetragonally with $Z = 2$ in the space group $P4/mbm$ with lattice constants $a = 952.6(1)$ pm and $c = 304.8(1)$ pm for $Sc_3Ir_5B_2$ and ranging from $a = 927.0(1)$ pm and $c = 296.8(1)$ pm ($Sc_2BeIr_5B_2$) to $a = 932.9(1)$ pm and $c = 310.3(1)$ pm ($Sc_2TiIr_5B_2$) for the quaternary compounds. According to powder diagrams, all compounds are isotypic. Structure determinations based on single-crystal X-ray data were performed for $Sc_2SiIr_5B_2$, $Sc_2VIr_5B_2$, and $Sc_2FeIr_5B_2$. $Sc_3Ir_5B_2$ crystallizes with the $Ti_3Co_5B_2$-type compounds, while the quaternary compounds form an ordered substitutional variant of this structure. The M atoms are arranged in rows along [001] with M−M distances of ∼300 pm in the rows and ∼660 pm between the rows. For the compounds with M = Mn, Fe, or Co, this results in highly anisotropic magnetic properties. Susceptibility measurements with a Faraday balance in the range 7−770 K suggest ferromagnetic coupling in the rows at low temperatures. Between the rows, the coupling was antiferromagnetic for $Sc_2FeIr_5B_2$ ($T_N \approx 190$ K) and ferromagnetic for $Sc_2MnIr_5B_2$ ($T_C \approx 115$ K, $\mu_s \approx 1.2\mu_B$) and for $Sc_2CoIr_5B_2$ ($T_C \approx 135$ K, $\mu_s \approx 1.2\mu_B$). The temperature dependence of the resistivity was measured for the compounds with M = Si, Mn, Fe, and Co.

Introduction

The interactions between chains of magnetically coupled atoms in nonmetallic compounds have been extensively studied. Little is known, however, about the corresponding metallic systems. We found that some classes of quaternary borides with well-separated rows of magnetically active 3d metals are suited for such investigations. Former studies on ternary and quaternary magnesium iridium borides resulted in the synthesis of a series of isotypic compounds $Mg_2MT_5B_2$, when T = Ir or Rh and M = Be, Al, Si, P, Ti, V, Cr, Mn, Fe, Co, Ni, Cu, Zn, Ga, Ge, or As,[1,2] all crystallizing with an ordered substitutional variant of the $Ti_3Co_5B_2$ type.[3] In this structure the M atoms are arranged in chains with M−M intrachain distances of ∼300 pm and interchain distances of ∼660 pm. For the compounds with M = Mn or Fe, this results in strong direct magnetic coupling in the chains and weak indirect coupling between the chains,[2] presumably via the long-reaching RKKY mechanism.[4−6] Considering the similarity in the crystal chemical behavior of magnesium and scandium in intermetallic compounds, we investigated the corresponding scandium systems. Here we report on the new compounds $Sc_3Ir_5B_2$ and $Sc_2MIr_5B_2$ in which M = Be, Al, Si, Ti, V, Cr, Mn, Fe, Co, Ni, Cu, Ga, or Ge. Investigations on similar series of scandium and magnesium compounds with rhodium and ruthenium instead of iridium are in progress and will be presented in a forthcoming paper.

Table 1. Lattice Constants (Guinier) of $Sc_3Ir_5B_2$ and the Compounds $Sc_2MIr_5B_2$ (SD < 0.1 pm)

	a, pm	*c*, pm	*V*, 10^6 pm^3
$Sc_3Ir_5B_2$	952.6	304.8	276.6
$Sc_2BeIr_5B_2$	927.0	296.8	255.0
$Sc_2AlIr_5B_2$	936.0	300.5	263.3
$Sc_2SiIr_5B_2$	922.7	306.9	261.3
$Sc_2TiIr_5B_2$	932.9	310.3	267.0
$Sc_2VIr_5B_2$	929.0	311.6	268.9
$Sc_2CrIr_5B_2$	937.3	306.4	269.2
$Sc_2MnIr_5B_2$	940.5	304.3	269.2
$Sc_2FeIr_5B_2$	937.3	302.8	266.0
$Sc_2CoIr_5B_2$	930.3	303.1	262.4
$Sc_2NiIr_5B_2$	922.1	309.5	263.2
$Sc_2CuIr_5B_2$	929.0	306.7	264.7
$Sc_2GaIr_5B_2$	935.2	303.9	265.9
$Sc_2GeIr_5B_2$	922.8	313.8	267.2

Experimental Section

Synthesis and Characterization. The title compounds were synthesized by arc-melting appropriate compressed mixtures of the elemental components from both sides in an argon atmosphere on a water-cooled copper plate and using a tungsten tip as a second electrode (scandium: 99.9%, pieces, Johnson Matthey; iridium: 99.9%, powder, Degussa; boron:

(1) Schiffer, J.; Jung, W. *Z. Anorg. Allg. Chem.* **1990**, *581*, 135.
(2) Nagelschmitz, E. A.; Jung, W. Manuscript to be published.
(3) Kuz'ma, Yu. B.; Yarmolyuk, Ya. P. *Zh. Strukt. Khim.* **1971**, *12*, 458.
(4) Ruderman, M. A.; Kittel, C. *Phys. Rev.* **1954,** *96*, 99.
(5) Kasuya, T. *Prog. Theor. Phys.* **1956,** *16*, 45, 58.
(6) Yosida, K. *Phys. Rev.* **1957,** *106*, 893.

10.1021/cm9802898 CCC: $15.00 © 1998 American Chemical Society
Published on Web 09/24/1998

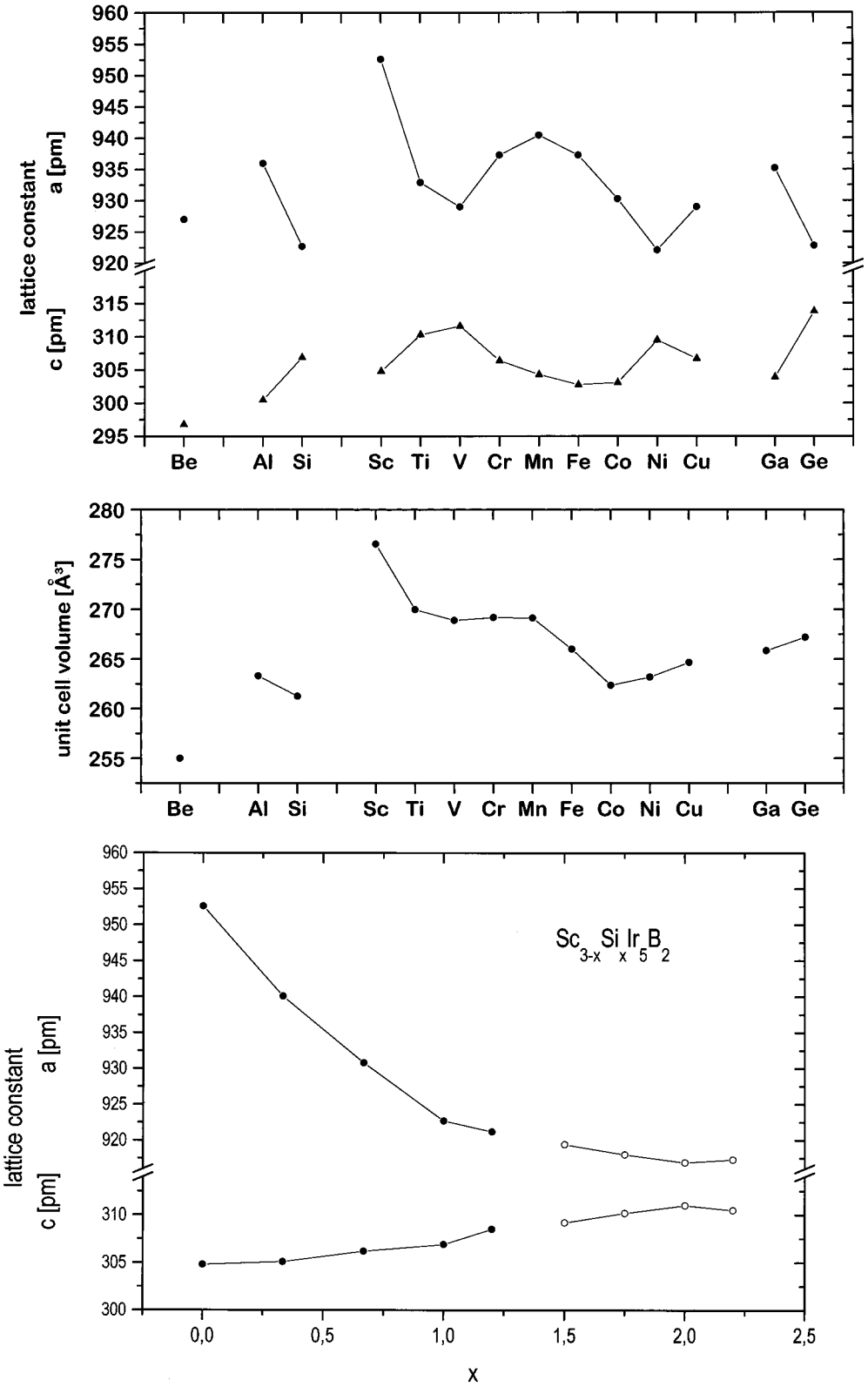

Figure 1. Quaternary compounds $Sc_2MIr_5B_2$ (tetragonal, *P*4/*mbm*). (Top) Plot of lattice constants *a* and *c*; (middle) plot of unit cell volume vs atomic number of M; (bottom) lattice constants *a* and *c* vs *x* for the tetragonal phase in samples with compositions $Sc_{3-x}Si_xIr_5B_2$ ($0 \le x \le 2.2$), which were single-phase in the range $0 \le x \le 1.2$ (●) and multiphase for $1.5 \le x \le 2.2$ (○).

99.9%, pieces, Aldrich; elements M: at least 99.9%). Weight losses during the melting process were negligible. Subsequently the pellets were annealed for 2 days at 1150 °C in an atmosphere of purified argon in alumina crucibles sealed in quartz glass tubes. Attempts to prepare the compound with M = Zn failed. Guinier powder diagrams of all compounds were recorded by using Cu−$K_{\alpha 1}$ radiation and Si as an internal standard. The diagrams were indexed tetragonally on the basis of single-crystal data. Most of the samples were single-phase. Only those with M = Ni or Cu were slightly contaminated by other phases. The lattice constants (Table 1) were obtained by least-squares fits of the powder data. Lattice constants and unit cell volumes are plotted versus the atomic number of M in Figure 1 (top and middle panels, respectively). Passing from Sc to Co, the unit cell volumes decrease, with an intermediate maximum at Mn, and thereafter increase from

Table 2. Crystallographic Data and Details of the Data Collection of $Sc_2SiIr_5B_2$, $Sc_2VIr_5B_2$, and $Sc_2FeIr_5B_2$ (tetragonal, space group *P4/mbm*)

	$Sc_2SiIr_5B_2$	$Sc_2VIr_5B_2$	$Sc_2FeIr_5B_2$
formula units per cell	2	2	2
crystal size (mm^3)	0.05 × 0.07 × 0.12	0.06 × 0.06 × 0.14	0.05 × 0.05 × 0.05
d_{X-ray} (g cm^{-3})	13.991	13.875	14.088
$d_{pyc.}$ (g cm^{-3})	14.02	14.11	−
θ_{max}	40°	40°	45°
scan width ($\theta-2\theta$, + 25% background)	0.6°	0.6°	0.9°
maximum measuring time per reflection (s)	90	180	90
number of measured reflections	3508	3596	4019
number of independent reflections	489	501	645
number of observed reflections ($I > 2\sigma_I$)	254	279	458
internal R (on F values)	0.117	0.133	0.102
number of variables	19	19	19
R	0.046	0.074	0.049
R_w ($W = 1/\sigma^2(F_o)$)	0.045	0.068	0.044

Co to Ge. As no systematic variations with the atomic radii of M could be observed, electronic reasons should be responsible for the volume change. Analysis of the variation of lattice constants with M reveals that in general if *a* goes up, *c* goes down, and vice versa. An exception is the series of compounds with the magnetically active metals M = Mn, Fe, or Co, where *a* and *c* go down simultaneously.

For M = Si, the whole range of compositions $Sc_{3-x}M_xIr_5B_2$ $0 \le x \le 3$ has been studied. Samples with $0 \le x \le 1.2$ were single-phase and showed a continuous variation of the lattice constants with *x* (Figure 1, bottom panel), indicating a range of homogeneity within these limits. The composition $Sc_2SiIr_5B_2$ is thus only a special point in the solid solution field. Whether this holds also for the other quaternary compounds has not yet been investigated. In the region above $x = 1.2$, the powder diagrams of the samples showed reflections of unknown phases that increased in number and intensity with *x*. Despite this, variation of the lattice constants of the tetragonal phase continued until the pattern disappeared between $x = 2.2$ and 2.5. Presumably because a change in the substitution mode, the composition of the tetragonal phase deviates from the sample composition at higher Si/Sc ratios. This part of the system needs further investigation.

Structure Determination. As judged from X-ray powder diagrams, all compounds listed in Table 1 are isotypic. Crystal structures were determined with single crystals of $Sc_2SiIr_5B_2$, $Sc_2VIr_5B_2$, and $Sc_2FeIr_5B_2$. Buerger precession photographs revealed tetragonal symmetry and the diffraction symbol $4/mmm\ P-b-$. X-ray intensity data were collected with a four-circle diffractometer (CAD4) using graphite-monochromated Mo−K_α radiation and corrected for absorption according to the crystal size. Crystallographic data and details concerning the data collection, the data reduction, and the structure refinements are given in Table 2. Because of the correspondence of diffraction symbol, lattice constants, and chemical composition isotypism with the $Mg_2MIr_5B_2$ compounds[1] could be assumed. Based on this model, the structures of the three compounds were refined in space group *P4/mbm* in the XTAL program system.[7] Final parameters are listed in Table 3. Interatomic distances up to 320 pm are given in Table 4.

Magnetic Susceptibility Measurements. We used a Faraday balance for making magnetic measurements on crushed samples of the compounds $Sc_2MnIr_5B_2$, $Sc_2FeIr_5B_2$, $Sc_2CoIr_5B_2$, and $Sc_2NiIr_5B_2$. Magnetization versus temperature data were taken in the range 7−770 K in magnetic fields up to 1.17×10^6 (A/m).

Resistivity Measurements. The electrical resistance of pressed and sintered (1150 °C) powdered samples of $Sc_2SiIr_5B_2$, $Sc_2MnIr_5B_2$, $Sc_2FeIr_5B_2$, and $Sc_2CoIr_5B_2$ was measured in the range 4.2−293 K by applying a dc four-probe method.

Results and Discussion

Crystal Chemistry. $Sc_3Ir_5B_2$ and the quaternary compounds $Sc_2MIr_5B_2$ crystallize with the $Ti_3Co_5B_2$-type structure[3] and a substitutional variant of this type, respectively. The latter was first established for $Mg_2SiIr_5B_2$.[1] For $Sc_2SiIr_5B_2$ as an example, the structure is shown as a projection along [001] in Figure 2. In the direction of the short axis, planar nets of iridium atoms at $z = 1/2$ composed of triangles, squares, and pentagons alternate with layers containing the boron, scandium, and M atoms at $z = 0$. By the stacking of the iridium nets, columns of triangular, tetragonal, and pentagonal prisms running along [001] are formed. While the triangular prisms are centered by boron atoms, the pentagonal and the tetragonal prisms in $Sc_3Ir_5B_2$ accommodate scandium atoms. In the quaternary compounds $Sc_2MIr_5B_2$, the scandium atoms residing in the tetragonal iridium prisms are completely replaced by

Table 3. Atomic Parameters of $Sc_2SiIr_5B_2$, $Sc_2VIr_5B_2$, and $Sc_2FeIr_5B_2$ (Space Group *P4/mbm*)

	$Sc_2SiIr_5B_2$	$Sc_2VIr_5B_2$	$Sc_2FeIr_5B_2$
Ir(1), 8j			
x	0.2121(1)	0.2162(2)	0.21664(6)
y	0.0698(1)	0.0706(2)	0.06927(7)
z	1/2	1/2	1/2
U_{11}	41(5)	98(6)	31(2)
U_{22}	50(6)	93(6)	44(2)
U_{33}	198(7)	178(8)	48(2)
U_{12} (pm^2)	−1(4)	−2(5)	−1(1)
Ir(2), 2c			
x	0	0	0
y	1/2	1/2	1/2
z	1/2	1/2	1/2
U_{11}	41(5)	97(7)	33(2)
U_{22}	U_{11}	U_{11}	U_{11}
U_{33}	13(1)	90(20)	52(3)
U_{12} (pm^2)	−5(8)	1(9)	−1(3)
Sc, 4g			
x	0.3252(7)	0.3240(8)	0.3234(3)
y	0.8252(7)	0.8240(8)	0.8235(3)
z	0	0	0
U_{11}	60(20)	80(20)	40(7)
U_{22}	U_{11}	U_{11}	U_{11}
U_{33}	20(4)	90(20)	42(10)
U_{12} (pm^2)	−30(20)	−20(30)	−12(10)
Si/V/Fe, 2a			
x	0	0	0
y	0	0	0
z	0	0	0
U_{11}	10(30)	10(20)	33(8)
U_{22}	U_{11}	U_{11}	U_{11}
U_{33}	2(70)	10(50)	48(13)
U_{12} (pm^2)	0	0	0
B, 4g			
x	0.123(4)	0.125(6)	0.124(2)
y	0.623(4)	0.625(6)	0.624(2)
z	0	0	0
U (pm^2)	40(8)	10(10)	98(39)

(7) Hall, S. R.; Stewart, J. M. XTAL 3.2; Universities of Western Australia and Maryland, 1989.

Table 4. Interatomic Distances of $Sc_2SiIr_5B_2$, $Sc_2VIr_5B_2$, and $Sc_2FeIr_5B_2$ up to 320 pm

		$Sc_2SiIr_5B_2$	$Sc_2VIr_5B_2$	$Sc_2FeIr_5B_2$
Ir(1)	Ir(1)	1 × 284.6(2)	1 × 279.5(2)	1 × 283.8(1)
		2 × 291.4(2)	2 × 298.0(2)	2 × 301.5(1)
		2 × 306.9(1)	2 × 311.21(7)	2 × 302.8(1)
	Ir(2)	1 × 273.3(2)	1 × 271.1(2)	1 × 273.4(1)
	Si/V/Fe	2 × 256.9(1)	2 × 262.0(1)	2 × 261.5(1)
	Sc	2 × 283.3(6)	2 × 284.1(7)	2 × 284.8(3)
		2 × 292.2(2)	2 × 294.0(7)	2 × 293.3(3)
	B	2 × 221.6(9)	2 × 220(4)	2 × 219(2)
Ir(2)	Ir(1)	4 × 273.3(2)	4 × 271.1(2)	4 × 273.4(1)
	Ir(2)	2 × 306.9(1)	2 × 311.21(7)	2 × 302.8(1)
	Sc	4 × 274.9(5)	4 × 278.3(7)	4 × 278.7(3)
	B	4 × 222(3)	4 × 226(4)	4 × 223(2)
Si/V/Fe	Ir(1)	8 × 256.9(1)	8 × 262.0(1)	8 × 261.5(1)
	Si/V/Fe	2 × 306.9(1)	2 × 311.21(7)	2 × 302.8(1)
Sc	Ir(1)	4 × 283.3(6)	4 × 284.1(7)	4 × 284.8(3)
		4 × 292.2(6)	4 × 294.0(7)	4 × 293.3(3)
	Ir(2)	2 × 274.9(5)	2 × 278.3(7)	2 × 278.7(3)
	Sc	2 × 306.9(1)	2 × 311.21(7)	2 × 302.8(1)
	B	1 × 264(4)	1 × 260(6)	1 × 264(2)
		2 × 279(4)	2 × 283(6)	2 × 286(2)
B	Ir(1)	4 × 222(3)	4 × 220(4)	4 × 219(2)
	Ir(2)	2 × 222(3)	2 × 226(4)	2 × 223(2)
	Sc	1 × 264(4)	1 × 260(6)	1 × 264(2)
		2 × 279(4)	2 × 283(6)	2 × 286(2)
	B	2 × 306.9(1)	2 × 311.21(7)	2 × 302.8(1)

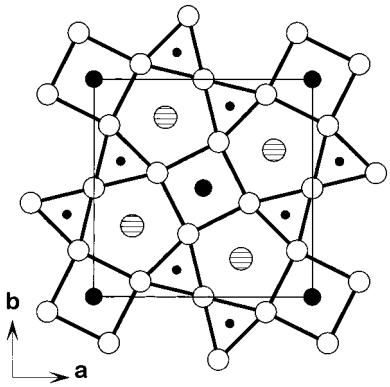

Figure 2. Structure of $Sc_2SiIr_5B_2$ (ordered substitutional variant of the $Ti_3Co_5B_2$ type structure), projection along [001]. (○), iridium at $z = 1/2$; all other atoms at $z = 0$. (•), boron; hatched circles, scandium; (●), Si in the case of $Sc_2SiIr_5B_2$ and Sc in the case of $Sc_3Ir_5B_2$.

M atoms (large filled circles in Figure 2). However, for M = Si, we found (Figure 1, bottom) that a solid solution $Sc_{3-x}Si_xIr_5B_2$ with $0 \le x \le 1.2$ exists. Apparently, a continuous substitution of silicon atoms for the scandium atoms in the tetragonal prisms and up to 10% of those residing in the pentagonal prisms is possible.

The columns of scandium-centered pentagonal iridium prisms in $Sc_2SiIr_5B_2$ may also be regarded as channels filled by chains of scandium atoms. The distance between the scandium atoms in the direction of the chain corresponding to the lattice constant *c* (307 pm) is significantly shorter than the metallic distance for CN 12 (324 pm). This holds also for the Sc−Ir distances, which range from 275 to 292 pm (average 289 pm), compared with a metallic radial sum for CN 12 of 298 pm. Only the Sc−B distance of 264 pm is slightly larger than the metallic radial sum for CN 12, 260 pm. If Pauling's bond length−bond strength formula[8] is applied with the usual value of 144 pm for the scandium metallic single-bond radius, the short distances between scandium and its neighboring atoms result in a bond-order sum of 7.5 at the scandium atom, which is far too large. So a reduction of the scandium radius related to some amount of charge transfer from scandium to the more electronegative elements in the compound may be assumed. Adjusting the metallic single-bond radius of scandium to 122.3 pm results in reasonable values for all bond-order sums: Sc, 3.00; Si, 3.95; Ir1, 4.64; Ir2, 6.10; B, 3.87.

(8) Pauling, L. *Die Natur der chemischen Bindung*; Verlag Chemie: Weinheim, 1964.

Table 5. Magnetic Parameters of $Sc_2MnIr_5B_2$, $Sc_2FeIr_5B_2$, and $Sc_2CoIr_5B_2$

$Sc_2MIr_5B_2$	M = Mn	M = Fe	M = Co
paramagnetic phase			
χ_o ($\times 10^{-8}$ m^3/mol)	–	4.9(1)	4.0(2)
Θ_p (K)	184(2)	241(1)	146(9)
C (m^3 $kmol^{-1}$)	$2.59(1) \times 10^{-5}$	$3.18(4) \times 10^{-5}$	$1.5(1) \times 10^{-5}$
μ_{eff} (μ_B/M atom)	3.76(1)	4.17(5)	2.9(1)
magnetically ordered phase			
T_C, T_N (K)	∼115 (T_C)	∼190 (T_N)	∼135 (T_C)
μ_s (μ_B/M atom)	∼1.2		∼1.2

[a] χ_o = Pauli term in the modified Curie−Weiss law $\chi = \chi_o + C/(T - \Theta_p)$; C = Curie constant; Θ_p = paramagnetic Curie temperature.

Magnetism. Of special interest are those $Sc_2MIr_5B_2$ quaternary compounds that contain magnetically active metals M such as Mn, Fe, and Co. These metal atoms are arranged in rows along [001] with distances of ∼300 pm in the rows and ∼660 pm between the rows. Therefore strong, direct magnetic interactions in the rows and weak, indirect interactions via the RKKY mechanism between the rows could be expected. To study these interactions, we investigated the magnetic behavior of the compounds with M = Mn, Fe, Co, and Ni in the range 7−770 K. The magnetic data are presented in Table 5.

$Sc_2NiIr_5B_2$ shows a temperature-independent Pauli paramagnetism with a molar susceptibility of $\sim 2 \times 10^{-8}$ (m^3/mol). The Mn, Fe, and Co compounds are paramagnetic at high temperatures and order magnetically at low temperatures. This may be seen from Figure 3 (a−c), which display the temperature dependence of the reciprocal susceptibility in the range 7−770 K. Two insets show the magnetization versus temperature for various field strengths (upper inset) and that versus applied magnetic field for various temperatures (lower inset) in the range 7−293 K.

For $Sc_2FeIr_5B_2$, the susceptibility is strongly field-dependent below ∼210 K (Figure 3a). The magnetization versus temperature curves (upper inset) reveal an

CN 14 is found for the two crystallographically independent iridium atoms (Ir1: 6 Ir, 4 Sc, 4 B; Ir2: 6 Ir, 4 Sc, 2 Si, 2 B). The Ir−Ir distances (273−307 pm, average 291 pm) are larger than in fcc iridium (272 pm) but short enough to be considered as bonding interactions. The average bond order according to Pauling's formula is 0.28. The shortest distances and probably the strongest bonds in the structure are those between the iridium and boron atoms. The boron atoms reside in triangular prisms formed by iridium atoms. The Ir−B distances of 222 pm compare with a covalent radial sum of 209 pm and a metallic distance for CN 12 of 234 pm and correspond to a bond order of 0.61.

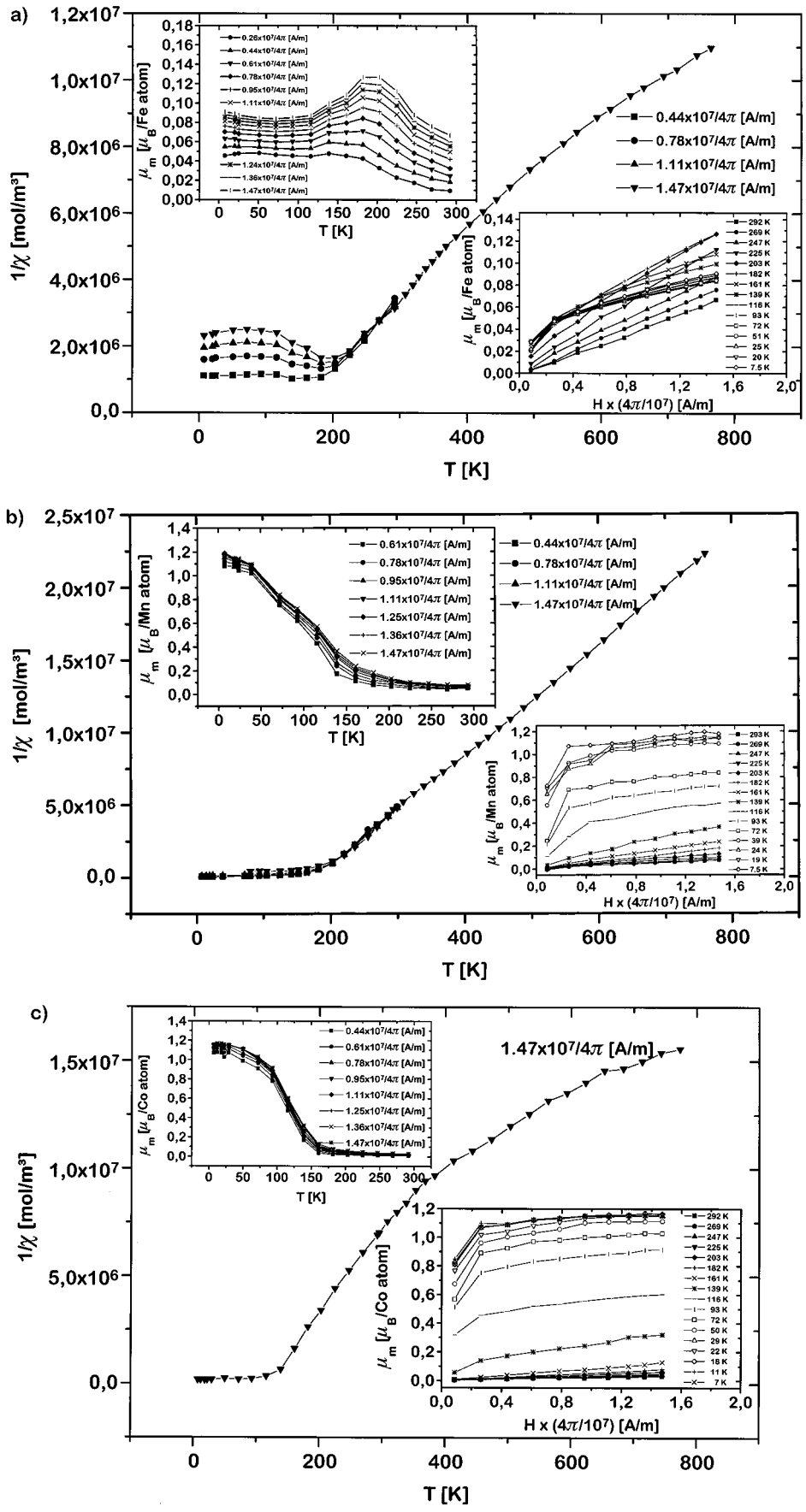

Figure 3. Inverse magnetic susceptibility vs temperature for (a) $Sc_2FeIr_5B_2$, (b) $Sc_2MnIr_5B_2$, and (c) $Sc_2CoIr_5B_2$. Upper insets: magnetization vs temperature for various field strengths. Lower insets: magnetization vs field strength for various temperatures.

antiferromagnetic transition with a Néel temperature of $T_N \approx 190$ K. Well above the transition temperature, the susceptibility becomes field-independent, following a modified Curie−Weiss law, $\chi = \chi_o + C/(T - \Theta_p)$, where

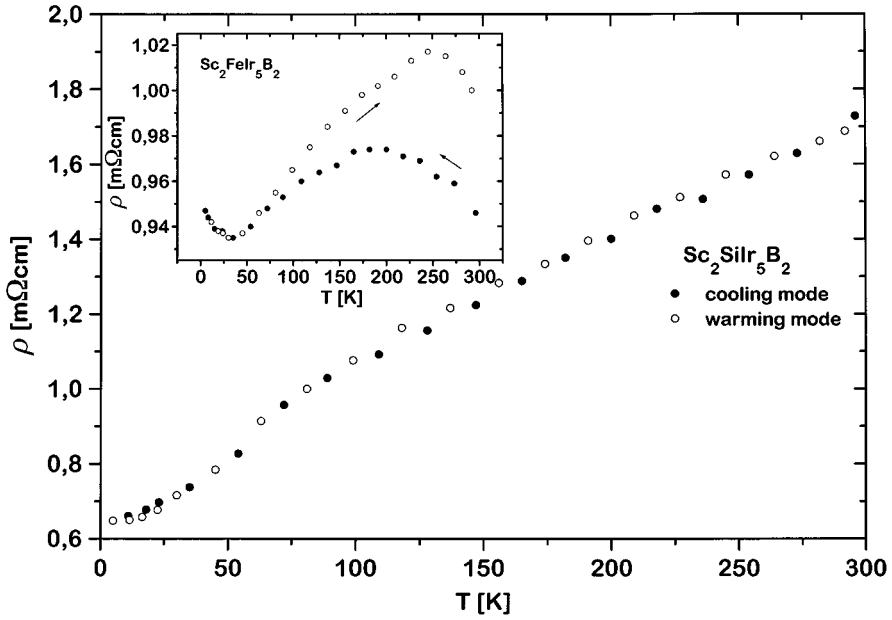

Figure 4. Temperature dependence of the electrical resistivity for $Sc_2SiIr_5B_2$. Inset: $Sc_2FeIr_5B_2$.

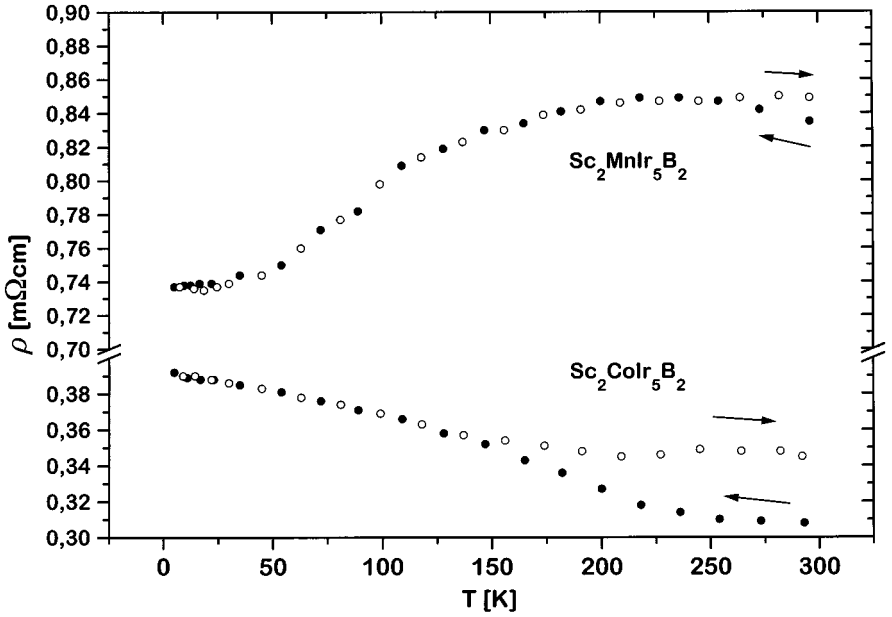

Figure 5. Temperature dependence of the electrical resistivity for $Sc_2MnIr_5B_2$ (upper part) and $Sc_2FeIr_5B_2$ (lower part). Symbols as in Figure 4.

χ_o is the temperature-independent Pauli term, C is the Curie constant, and Θ_p is the paramagnetic Curie−Weiss temperature. These parameters, evaluated from a least-squares fit in the region 300−770 K, are listed in Table 5. From the Curie constant an effective moment of μ_{eff} = 4.17(5) (μ_B/Fe atom) is calculated. Despite the observed antiferromagnetic transition, the paramagnetic Curie−Weiss temperature has a positive value (Θ_p = +241(1) K), which is indicative of predominantly ferromagnetic coupling. We may thus assume that the strong, direct intrachain interactions are ferromagnetic, while the weaker, indirect interchain interactions are antiferromagnetic. Verification of this model by neutron diffraction is in progress.

The magnetic data of $Sc_2MnIr_5B_2$ are depicted in Figure 3b. Above 350 K, the reciprocal susceptibility is seen to behave according to the Curie−Weiss law. The effective moment derived from the slope of the $\chi^{-1}(T)$ curve equals 3.76(1) (μ_B/Mn atom), which is close to the spin-only value of 3.87 μ_B expected for a system with S = 3/2. The Curie−Weiss intercept Θ_p is equal to 184-(2) K. Magnetization versus temperature curves (upper inset) suggest a ferromagnetic transition. At 7.5 K and an applied field of $1.47 \times 10^7/4\pi$ (A/m), a saturation moment of $\mu_s \approx 1.2$ (μ_B/Mn atom) is reached (lower inset). The Curie temperature determined by the method of Belov and Kouvel[9,10] is $T_c \approx 115$ K.

Figure 3c summarizes the magnetic data of $Sc_2CoIr_5B_2$. No Curie−Weiss behavior is observed at temperatures up to 770 K. Therefore the paramagnetic parameters (Table 5) had to be evaluated from a least-squares fit to the modified Curie−Weiss law by using a temperature-independent term, $\chi_o = 4.0(2) \times 10^{-8}$ (m^3/mol). The effective magnetic moment of μ_{eff} = 2.9(1) (μ_B/Co atom) calculated from the Curie constant is close to the spin-only value of a system with S = 1 (2.83 μ_B).

Again, ferromagnetism is observed at low temperatures (upper inset) with a Curie temperature T_C of ~135 K, as determined by the Belov and Kouvel method. The saturation moment (lower inset) approaches 1.2 (μ_B/Co atom) at 7 K in a field of $1.47 \times 10^7/4\pi$ (A/m).

Electrical Conductivity. For $Sc_2SiIr_5B_2$ the temperature dependence of the resistivity is presented in Figure 4. As expected for a metallic compound without magnetic ordering, the resistivity decreases monotonically with decreasing temperature. The behavior of $Sc_2FeIr_5B_2$ (inset in Figure 4) is quite different. Upon cooling, the resistivity goes through a maximum at the Néel point. Upon warming, the resistivity rises to higher values and the maximum is shifted toward higher temperatures. No explanation can be given for this phenomenon at the moment. The increase of the resistivity below ~30 K is possibly caused by Kondo scattering attributable to a small amount of paramagnetic Fe atoms statistically distributed on Ir sites. The resistivity of $Sc_2MnIr_5B_2$ (upper part of Figure 5) decreases upon cooling after a shallow maximum at 220 K. The nonlinear behavior may be due to interband scattering of the conduction electrons.[11] In its lower part, Figure 5 shows the $\rho(T)$ dependence for $Sc_2CoIr_5B_2$. Unexpectedly, the temperature coefficient for the cooling mode is negative over the whole temperature range studied. Again, upon warming, a different $\rho(T)$ behavior with a maximum at ~270 K is observed.

Acknowledgment. Financial support from the Deutsche Forschungsgemeinschaft and the Fonds der Chemischen Industrie as well as a generous gift of iridium by the Degussa AG is gratefully acknowledged. Thanks are due H. Schumacher for skillful experimental work and electrical and magnetic measurements.

CM9802898

(9) Belov, K. P. *Magnetic Transactions*; Technical Publications: Boston, 1965; p 34.
(10) Kouvel, J. S.; Fisher, M. E. *Phys. Rev.* **1965,** *136,* A1626.
(11) Mott, N. F. *Adv. Phys.* **1964,** *13,* 325.